Null-Results of a Superconducting Gravity-Impulse-Generator

I. Lőrincz*and M. Tajmar†

Institute of Aerospace Engineering, Technische Universität Dresden, 01307 Dresden, Germany

It was claimed by Podkletnov and Modanese[1] that a high voltage discharge through a high-Tc superconductor produces a gravity-like beam that can be measured using pendulums up to 150 m away from the apparatus. As this would be of interrest for countless different applications, among them a beamed propulsion concept,[2] it has drawn a lot of attention. Recently Poher[3] and Schroeder[4] designed their own experimental setup to replicate a similar effect. In these experiments similar results were reported while using a high current direct discharge through a high-Tc superconductor. Additionally to the emitted gravity-like field that was measured with an accelerometer inside a Faraday-shield in close proximity of the superconductor, Poher also measured a mechanical impulse during the discharge. We previously performed two small scale experiments,[5] with the objective to replicate the reported results and to gather experience. We successfully replicated the mechanical impulse, but we could not generate repeatable gravity like signals. Since our previous results were inconclusive we decided to increase the impulse energy by at least an order of magnitude. We achieved this by replacing our previous capacitors[5] and their charging sub-system, reaching a theoretical maximum impulse energy of up to 0.25 MJ. Our first objective within the present series of experiments was to exclude the most important error source, which was the emitted electromagnetic pulse that greatly influenced the sensors and data acquisition systems. After this was achieved we investigated the cause of the mechanical impulse, which led eventually in every case to the destruction of the emitter and its support. We could measure no acceleration change during the discharges within our 3σ limit of ± 48 μg and thus setting a new lower limit for similar effects.

I. Introduction

A. Background

The experimental connections between superconductors and gravity-like fields started with the publication of the unexpected findings of E. Podkletnov and R. Nieminen[6] in 1992 while a ceramic high-temperature superconductor disc was rotated by using pseudo-rotating magnetic fields. The authors reported a weight loss of a proof mass placed above the disc dependent on its rotational speed. Numerous follow-up experiments were published since with different experimental configurations having the commonality of generating a supercurrent with a superconductor disk and investigating whether this would lead to an emitted gravity-like field. Two examples of these experiments can be seen in Figures 1 and 2.

In Figure 1 a schematic is shown in which an electric discharge between a superconductor disc and an electrode is performed, emitting the claimed gravity-like field and causing the movement of a pendulum placed at a distance of up to 150 m. In this design the reported discharge voltage, supplied by a Marx-generator, reached values of up to 200 kV and produced peak current of up to 10 kA between a normal metal electrode and a HTSC disc, in which magnetic fields of up to 0.5 T were trapped. The electrodes were placed in a cylindrical evacuated enclosure while the distance between them could be varied from 0.15 to 0.40 m. With this assembly Podkletnov observed a radiation beam emitted along the discharge's axis that showed gravitation like properties. The discharges between the electrodes were focused with a solenoid wound around the chamber to optimize the reported effect. It was claimed that the impulses measured with the pendulums

*PhD Student, E-Mail: istvan.lorincz@tu-dresden.de, Student Member

†Professor, Institute Director and Head of Space Systems Chair, E-Mail: martin.tajmar@tu-dresden.de, Senior Member

were not attenuated by obstacles (e.g. brick walls) and were not divergent within the measurement's range. The amplitude of the pendulum's horizontal deflection was reported as being independent of the material and proportional to the mass of the sample.

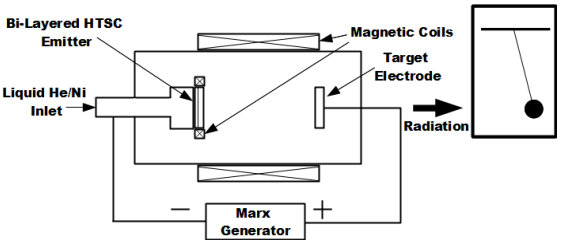

Figure 1. Schematic of Podkletnov's experimental setup[1]

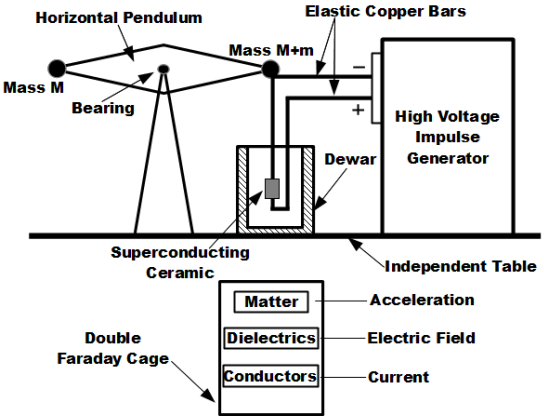

Figure 2. Schematic of Poher's Experimental setup and sensor arrangement[3]

In Figure 2 the setup of Poher[3] is shown, in which both of the electrodes are in contact with the superconductor disc's surface. During an electric current impulse generated by a capacitor bank a similar effect was observed that was measured with accelerometers placed co-axially below the superconductor disc. In addition to the emitted field a recoil of the superconductor was observed, which was claimed to be the result of the emitted field. In their paper, Poher et al. describe a relatively simple setup for generating high voltage (up to 4 kV) DC discharges through the emitters. The current was generated by the discharge of a 47 μF capacitor connected in series with the emitter. The measurement of the recoil was done by a horizontal pendulum (Figure 2.) above the emitter while the gravity like flux was measured below in a double Faraday cage with a non-ferromagnetic mass attached to a piezoelectric sensor at a distance of 26 cm from the emitter. Other sensors were also placed in the enclosure together with the accelerometer in order to measure the electromagnetic properties of the emitted fux and possible unwanted EM radiation. With these sensors both phenomena -recoil and fux- could be characterized. In the published results a maximum acceleration of the test mass of approx. 0.125 m/s2 (0.0127 g) was measured[7] during a discharge of 2900 V and an estimated peak current (based on the derived total resistance of the circuit) of 6900 A through an unspecifed type of emitter (designated EM42). A more detailed analysis and comparison between the experiments of Podkeltnov and Poher was already published by Modanese.[8]

Besides Poher's publications a much more extensive overview of his experiments and methods can be found online[9] in form of a journal, in which the various emitter types are described. Based on the data found in the journal the conclusion can be drawn that in order to maximize -at least- the recoil effect, the emitters have to be as thin as possible and stacked on one another. He also states that the emitted flux is highly divergent and thus the sensor's projected area and distance from the emitter are crucial in the characterization process. The results of a measurement series in which the stacked piezoelectric sensor with an attached mass (of 0.687 x 10^{-3} kg) is shown in Table 1.

Five different types of sensing techniques were applied in order to try to distinguish between the claimed flux and other influencing factors like acoustic and EM noise:

1. piezoelectric sensor with a test mass (0.687 x 10^{-3} kg) attached on top
2. microphone
3. speaker/voice coil
4. light reflection on water surface
5. commercial accelerometer (11 kHz resonance) - A/120/VT/N from "DJB instruments"

Another independent test series was conducted by Schroeder,[4] in which a reproduction of Poher's experiments was attempted. In his setup, Schroeder connected a 1 inch diameter YBCO disc in series with a

Table 1. Poher's measurement results[9] of the claimed gravity like flux from a series of discharges through a stacked emitter, measured by the piezoelectric sensor with a sensitivity factor of 0.07 m/s^2/mV (0.0071 g/mV)

Discharge Voltage [V]	Discharge Energy [J]	Piezo Accelerometer [mV p-p]	Acceleration [mg]
1500	232	5.76	41.11
1900	373	7.60	54.25
2266	530	10.00	71.38
2575	685	7.92	56.53
2884	859	11.70	83.51

capacitor bank, which could deliver currents of up to 2 kA at 1 kV. He reported that a 1kV impulse produced an acceleration signal of approx. 0.00981 m/s2 (0.001 g), which disappeared if the disc was above its critical temperature. For a more detailed description of the experiments and the history of this topic the reader is referred to our previous paper.[5]

Since the setup used by Poher is simpler than the setup described by Podkletnov, but still based on the same principle we decided to reproduce the setup of Poher. Eventhough Poher applies superconductor emitters that are stacked and custom made, it was claimed that the effect is also measurable with normal bulk YBCO discs, as was also the case in Schroeder's reproduction.

B. Our First Trials

In our previous trials we set out to gather experience by building a small scale impulse generator, with which we could deliver current impulses of up to 1 kA, after which a new impulse generator was built that delivered impulses of up to 9 kA with a duration of up to 150 microseconds. In Figure 3 the schematic of our first setup is shown.

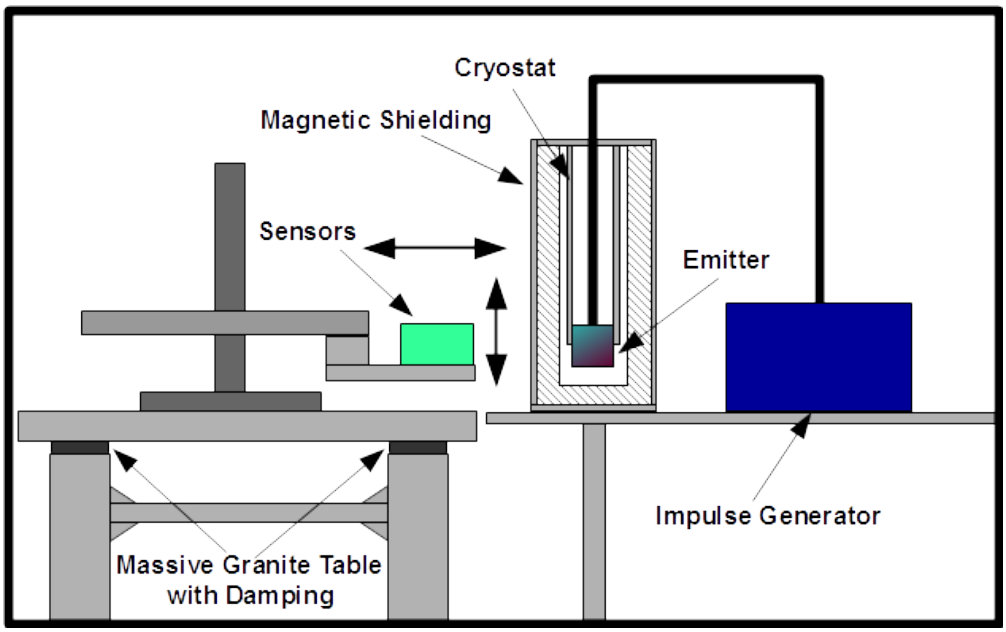

Figure 3. Schematic of our first experimental setup[5]

We applied two methods to generate a supercurrent, first by a direct current discharge through the superconductor disc and secondly through a magnetic field, for which the schematics are shown in Figures 4 and 5 respectively.

After perfoming numerous measurements with two types of superconductor discs and three different types of sensors (MEMS accelerometer: Colibrys - SF1500SN.A , piezoelectric vibration sensor: PCB-352C33 and

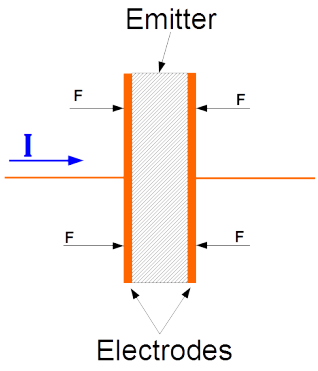

Figure 4. DC configuration

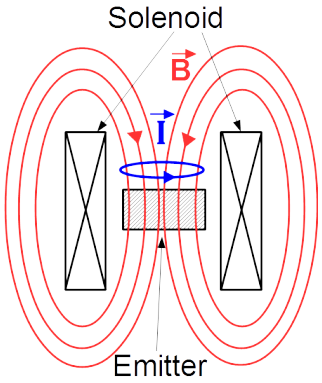

Figure 5. Magnetic field induced current configuration

a custom built optical accelerometer[5]) the conclusions drawn were inconclusive.

Based on the previously published results of Poher[7] and Schroeder,[4] we set our expected minimum acceleration magnitude to 0.00981 m/s^2. Unfortunatelly due to the equipment and the emitted electromagnetic pulse (EMP) we could not achieve this sensitivity in our measurements. We had three major problems, due to which we could not achieve the required sensitivity:

1. The impulse duration was too short for the MEMS accelerometer
2. The EMP influence was too high for the piezoelectric vibration sensor and the MEMS accelerometer
3. The sensitivity of the optical accelerometer was too low

C. Objectives for the Second Trials

In order to meet our requirements, a follow-up series of experiments was inevitable. Our first and most important objective was to shield the sensor equipment from the EMP, which would allow us to acurately measure acceleration signals with an amplitude below 0.5 mg at frequencies of up to 60 kHz with our vibration sensor.

Further we observed and measured a significant acoustic signal during impulses through the superconductors. Our next objective was to find an explanation that was necessary to provide a satisfactory conclusion, since it was previously claimed by Poher[3,10] that this effect is a direct consequence of the emitted gravity-like field.

Our last objective was to increase the impulse duration (approx. 150 μs) by at least an order of magnitude to test also the possibility that only a small percentage of the actual electric current impulse produces a measurable field by our equipment as assumed by Poher. If this were the case, while assuming the worst case scenario that only 10% of the current impulse's duration produces a measurable acceleration amplitude,[9] the frequency of the acceleration signal would be beyond our sensor's range. Hence by increasing the duration by an order of magnitude, the expected signal would fall back into our measurable range of 0-60 kHz.

We have also decided that for the second trials we only apply the DC configuration (Figure 4), since this leads to the highest supercurrent amplitude and generates also a significantly weaker EMP compared to the magnetic field induced current configuration. In addition to this, the expected direction of the emited gravity-like field corresponds to the direction of the current through the superconductor, which makes the DC configuration the better choice for coaxial acceleration measurements.

II. Experimental Setup

A. Electromagnetic Shielding Upgrade

We have built a large double shielded Faraday cage in which the vibration sensor equipment could fit, including its data aquisition (DAQ) system. The synchronization of the accelerometer and the impulse generator was achieved by optically triggering the two separate DAQs with a 2mm diameter optical cable,

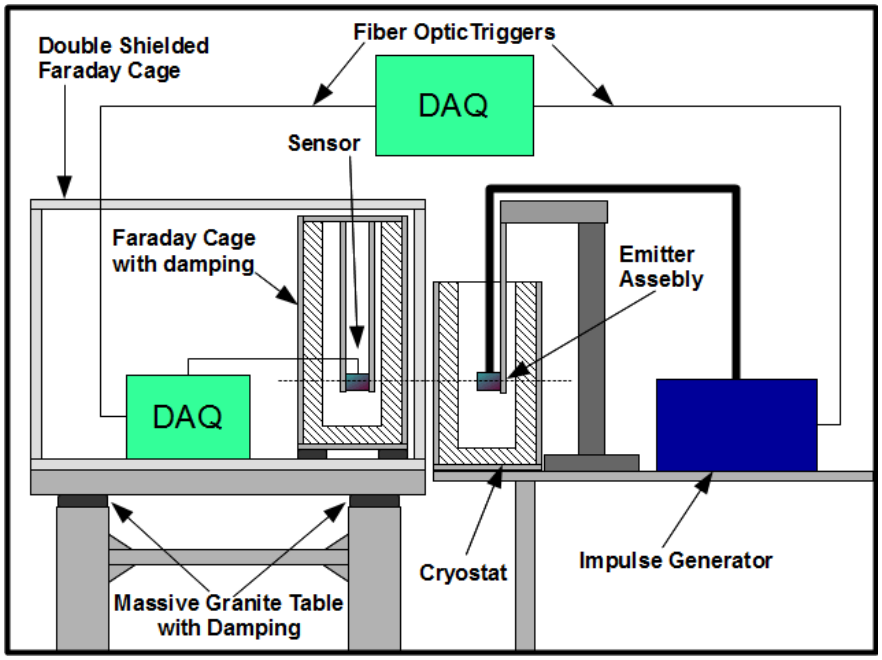

Figure 6. Schematic of our upgraded experimental setup

which was the only connection between the outside environment and the inside of the Faraday cage. Another Faraday cage was built for the impulse generator that shielded the high intensity current impulse's path. To maximize the EMP damping, the current impulse was lead towards the outside through a coaxial cable, thus leaving only the emitter assembly (electrodes and superconductor) as a significant source for an EMP. After a few trials with this setup we still saw an EMP influence on the accelerometer, so we applied copper tape to the edges of both Faraday cages, which further improved the damping. Even with these careful improvements the EMP influence was still measurable in the range of up to 1-2 mg on the accelerometer. Hence we placed a third Faraday cage made out of soft iron (with a high magnetic permeability) inside the double shielded box. We placed the accelerometer and its amplifier inside the third box while leaving the DAQ system outside (within the double shielded box). Finally we could achieve a damping that decreased the EMP influence on our sensor below its sensitivity. The schematic of our final experimental setup can be seen in Figure 6.

B. Impulse Generator and Data Aquisition System

We had to change the procedure for generating an impulse and aquiring the data in order to synchronize two separate data aquisition systems. We achieved this through setting up an optical triggering system, controlled by an arduino. The simplified schematic of our electronic subsystems can be seen in Figure 7. The dashed lines represent the high current impulse's path. We used a spark gap between two metal spheres as a switch, where one of the spheres was moved by a stepper motor in order to control the gap distance. During the charging of the capacitor bank the gap was increased beyond the voltage breakdown limit. After the required voltage was reached the stepper motor was started to decrease the gap distance and after a small delay the DAQs were triggered simultaneously. After we calibrated the triggering system, we achieved a synchronization error below the impulse generator's DAQ time resolution (4μs).

C. New Emitter Assembly

During our first trials the emitter assembly was held together by 3D printed parts, which were all eventually destroyed during the impulses. In order to overcome this problem we made a new emitter assembly, which would withstand even the most powerful impulses at LN2 temperatures. A schematic of the emitter assembly can be seen in Figure 9.

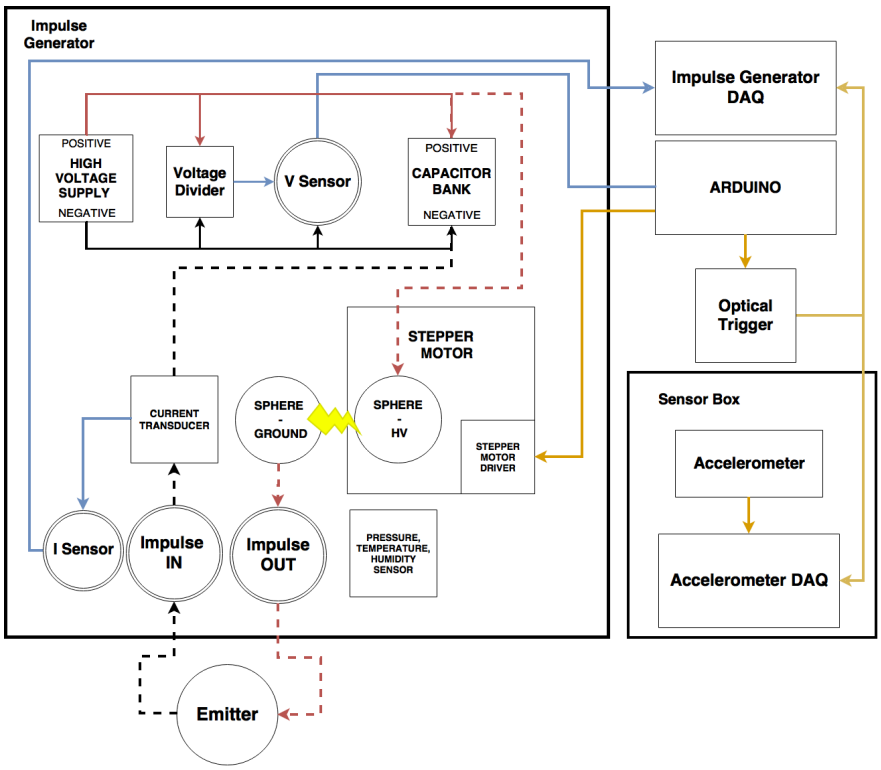

Figure 7. Simplified schematic of the electronic subsystems.

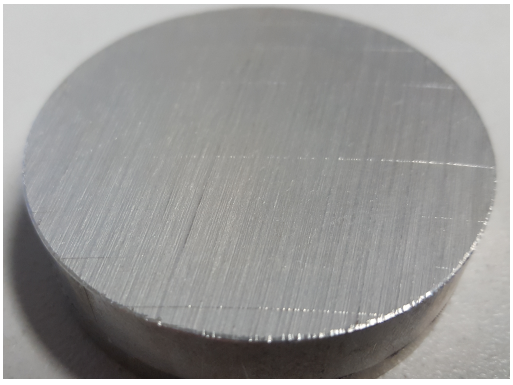

Figure 8. The surface of the hollow aluminium dummy emitter. The increased roughness of the surface should trap small ammounts of liquid nitrogen, which could quickly evaporate during the impulses due to joule heating

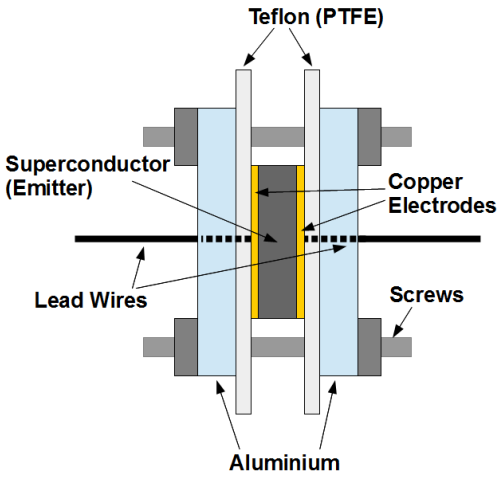

Figure 9. Schematic of the emitter assembly for the copper disc electrodes. The superconductor is simply pressed together between the electrodes. The necessary stiffness for the whole assembly is provided by the relatively thick aluminium discs.

D. Electrode Geometries

We made measurements with two different electrode types. First we used two 1 mm thick copper plates between which the superconductor was pressed and secondly we made two pairs of electrodes that had inside a hollow paraboloid shape (Figure 10). With the paraboloid geometry only the edges of the superconductor discs were connected to the electrodes, which lead to a different interaction between the induced magnetic fields of the electric currents flowing through the emmitter assembly as compared to the case with the flat disc electrodes. Thus we could observe if the acoustic signal would change, in case of which the conclusion that it is due to a magnetic interaction would be supported.

E. Impulse Duration Upgrade

First we perfomed impulses with our previous capacitor bank that had a capacitance of 200 μF[5] to have a baseline for comparison. After that we upgraded the impulse generator to achieve a longer current impulse. The most obvious way to increase the duration of the impulse is by increasing the total capacitance of the impulse generator. We obtained three large capacitors, which were custom made for high power impulse generators. Each capacitor had a capacitance of 1660 μF $\pm$10%, rated voltage of 10 kV and rated peak current of 60 kA. If connected in parallel the impulse generator could store a maximum total energy of 0.249 MJ at 10 kV charge voltage. The charger of the impulse generator was also upgraded to a high voltage power supply capable of delivering 5 A at 10 kV, this reduced the charging time by up to 3 orders of magnitude compared to our previous setup.

Figure 10. The paraboloid electrodes inside their polyamide insulation with the 45 mm diameter sigle-crystal YBCO superconductor disc (right). The small seed crystal can be seen in the middle of the disc.

Although we have planned to use all three capacitors in parallel for all our measurements, we have determined after a few trials that the energy released into our superconductors would be too much (the reasons will be explained in the next chapter). Thus we have decided to use only one of the three large capacitors.

F. Superconductor Disc Types

We used three types of YBCO superconductor discs:

1. Two discs with diameters of 31.5 mm and 45 mm (Figure 10) and approximately 3 mm thick, each grown from a single crystal source.
2. A single disc grown from five crystal sources (Multi-Crystal) with a diameter of 47 mm and a thickness of approximately 4 mm.
3. A sintered disc with a 44 mm diameter and a thickness of 5 mm.

III. Experimental Results

All of the measurements were performed while the sensor was coaxially aligned with the rotation axis of the superconductor discs at distances of 25 and 50 cm. For the orientation of the rotation axis we chose to perform impulses in the horizontal and then in the vertical direction (with the sensor below the emitter). Finally the last parameter that we varied was the electric current flow's direction relative to the sensor, either towards or away from the sensor, which we defined as the positive and negative impulse direction.

A. Control Experiments

The control measurements for our first setup were made with an aluminium disc in air and liquid nitrogen (LN2) as well as with the superconductors in air. In our first trials we observed a higher intensity acoustic signal during the impulses through the superconductor in LN2 compared to the control measurements. The most obvious possible reason for this effect was an interaction between the induced magnetic field by the current flowing in the connecting wires of the electrodes and the surface currents of the superconductor. For this reason we made a "dummy" emitter out of aluminium that was hollow inside, having only a 1 mm wall thickness.

Furthermore gas bubble release was also observed during the impulses through the superconductors, but we could not determine the origin of these with a satisfactory certainty. Hence the surface roughness of the hollow aluminium disc (Figure 8) was increased until it allowed small ammounts of LN2 to be enclosed between the aluminium disc and and the electrodes. Through this we could investigate whether contact imperfections would lead to an increase in localized electrical contact resistance, which in turn would lead to the vaporization of the LN2 enclosed between the electrodes and the aluminium disc during the current impulses. If this were the case, the gas bubbles formed between the electrodes and the superconductor due to the highly localized Joule heating could indeed lead to the observed increased acoustic signal and the previously reported recoil effect.

B. Small Capacitor Bank

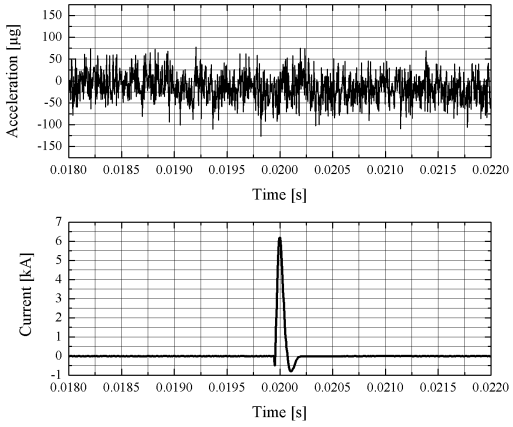

Figure 11. Control measurement with the vibration sensor and the hollow aluminium disc in LN2, pressed between two copper plates, during a discharge of the 200 μF capacitor bank charged to 1800 V. No EMP influence and also no acoustic signal was measured.

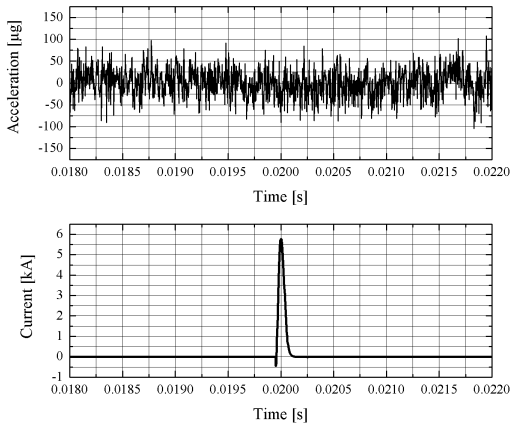

Figure 12. Control measurement with the vibration sensor and the sintered YBCO disc, pressed between two copper plates, during a discharge of the 200 μF capacitor bank charged to 1800 V. No EMP influence and also no acoustic signal was measured.

For each experiment configuration we performed impulses through the hollow aluminium disc in air at room temperature and in LN2. A second control was also made with the superconductor discs in air at room temperature. We observed no increase in the acoustic signal and also no gas bubble release during impulses through our hollow aluminium dummy emitter in LN2. A measurement result (while in LN2) can be seen in Figure 11, where the 200 μF capacitor bank was discharged at a voltage of 1.8 kV delivering a current peak of 6.2 kA with a total impulse duration of 155 μs. As we can see in the vibration sensor's data no EMP influence was detected and also no measurable acoustic signal followed the current impulse. Through data processing a 3σ value of 100 μg could be achieved.

A measurement result with the same impulse parameters can be seen in Figure 12 with the sintered superconductor disc at room temperature in air. The vibration sensor data shows no change during the measurement. The same measurements were repeated with all the superconductor discs and both type of electrodes. All of the measurements showed no change in the sensor readout, through which we achieved our best control measurement series until now.

An overview of all the measurement results with the superconductors in LN2 and below Tc can be seen

in Table 2. In order to decrease the standard deviation (σ) of the measurements we signal averaged two impulses and then performed a downsampling with a factor of 4.

1. *Large Capacitor Bank*

The first impulses with the three large capacitors connected in parallel were made through the hollow aluminium disc. Based on our previous experience, we quickly realized that even at a voltage of 500 V the power of the discharge would shatter the superconductors, thus we decided to use a single large capacitor and keep the voltage below 1500 V. During the control measurements with a superconductor at room temperature, we could observe sparks originating from the contact region between superconductor and electrode. To analyze this effect we made video recodings, out of which we show two frames in Figure 13.

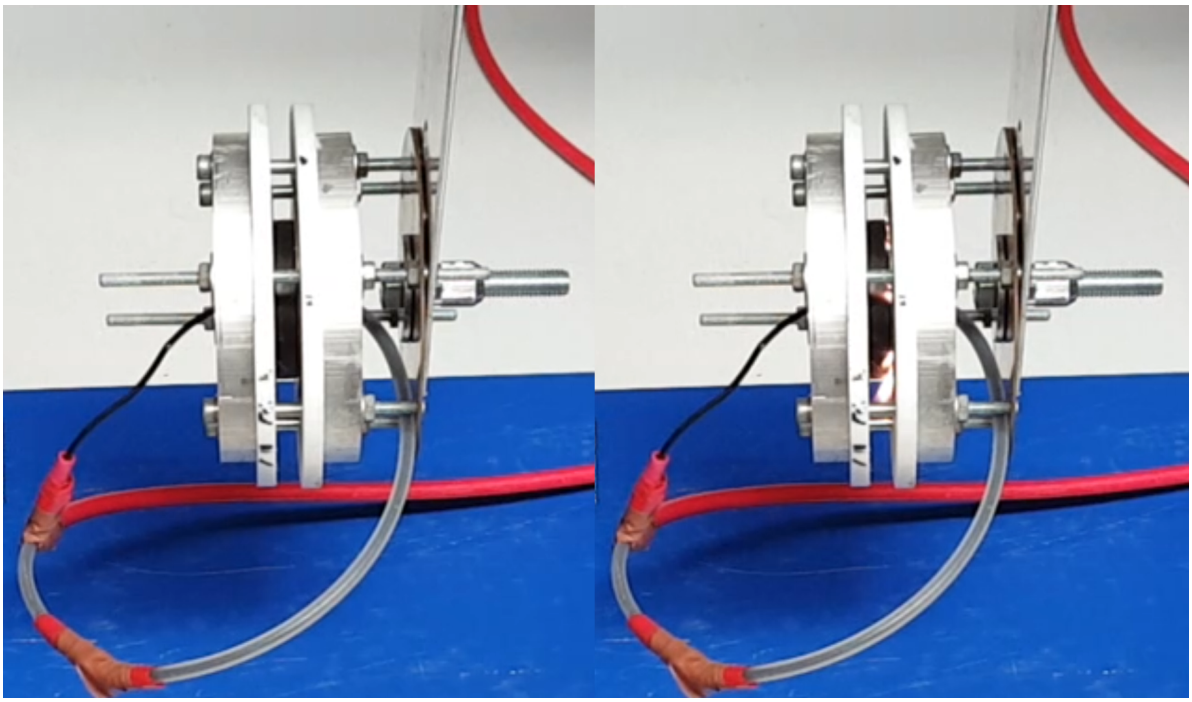

Figure 13. Two frames of a video recording during an impulse through the sintered superconductor disc. Left: Before the impulse. Right: During the impulse. We can clearly see the sparks inside the contact region between the superconductor and the cathode, causing erosion and radial matter ejection

On the left side we can see the normal state of the emitter assmebly, with the sintered superconductor in the middle and on the right side we see a frame during the impulse. We can clearly see sparks inside the contact region, which also show that material is being radially ejected during the impulses. This is also supported by the analysis of the superconductor's surface after the measurements were done. In Figure 14 we can see the sintered superconductor's surface after numerous impulses were performed in air and LN2, that shows clear signs of surface erosion. This observation leads to the conclusion that the observed gas bubbles in LN2 are generated by the heat released by the spark erosion of the superconductor's surface. This also causes a mechanical impulse in the support structure of the emitter assembly as the evaporated LN2 expands inside and around the contact region. This mechanical shock explains why our previous emitter assemblies including superconductors were destroyed during the impulses. As a first order approximation we calculated the ammount of heat necessary to generate the observed gas volume through vaporization of LN2. We could then derive the equivalent contact resistance that would create this heat through Joule heating:

- **N2 Gas Temperature:** $\mathrm{T} = 77\ \mathrm{K}$
- **N2 Gas Pressure:** $\mathrm{p} = 10^5\ \mathrm{Pa}$
- **Specific Gas Constant:** $R_s p = 0.351\ \frac{J}{gK}$

- **N2 Gas Density:** $\rho = \frac{p}{R_{sp}T} = 3694.37$ g/m^3
- **Evaporated gas volume:** V = 1.13x10^{-4} m^3
- **Mass of the evaporated gas:** $m_g = \rho$ x V = 0.42 g
- **Heat of vaporization of nitorgen at 77.36 K:** $\Delta H_{vap} = 199.26$ J/g
- **Total energy required to evaporate the gas:** $Q_{vap} = \Delta H_{vap}$ x $m_g = 83.2$ J
- **Total capacitance:** C = 200 μ F
- **Discharge voltage:** U = 2200 V
- **Total energy stored in capacitor:** $E_{tot} = \frac{1}{2}$ x C x $U^2 = 484$ J
- **Equivalent resistance that produces 83.2 J through Joule heating:** 0.035 Ω

The calculated equivalent resistance that would produce the heat necessary to evaporate the observed gas volume makes up only about 10% of the impulse circuit's total resistance, which is a realistic value. Hence we have found the cause to why our emmitter assemblies were broken apart during our first experiment series.

Figure 14. The eroded surface of the sintered superconductor disc, through which numerous impulses were performed in air and LN2

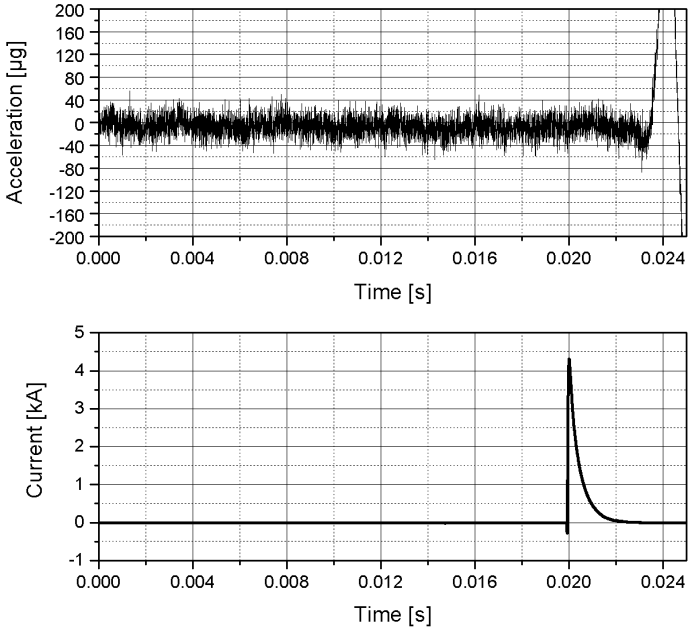

Figure 15. The average of five discharges of the large capacitor charged to 1.3 kV, through the sintered superconductor disc in liquid nitrogen

An overview of all the measurement results with the superconductors in LN2 and below Tc can be seen in Table 3. In order to further decrease the standard deviation (σ) of the measurements we signal averaged five impulses and then performed a downsampling with a factor of 4. In Figure 15 a measurement result is shown for the first configuration listed in Table 3, here we can also see the beginning of the acoustic signal (reaching offscale values) after the impulse. As we can see in the lower graph, the total current impulse duration has been increased to 2 ms. The duration of the current peak's top 10% is above 160 μs, fulfilling our objective of 150 μs.

Table 2. Results summary of the impulses performed with the 200 μF capacitor bank through the superconductors in liquid nitrogen. The acceleration standard deviation varies in the first decimal place, which is not shown.

Electrode Type	S/C Type	Orientation	Impulse Direction	Distance [cm]	Voltage [kV]	Discharge Energy [J]	Acceleration (3σ) [μg]
Copper Disc	Sintered	Horizontal	Positive	25	1.8	324	$\pm$ 100
Copper Disc	Sintered	Horizontal	Positive	50	1.8	324	$\pm$ 100
Copper Disc	Sintered	Horizontal	Negative	25	1.8	324	$\pm$ 100
Copper Disc	Sintered	Horizontal	Negative	50	1.8	324	$\pm$ 100
Copper Disc	Multi-Crystal	Vertical	Positive	25	2.2	484	$\pm$ 100
Copper Disc	Multi-Crystal	Vertical	Positive	50	2.2	484	$\pm$ 100
Copper Disc	Multi-Crystal	Vertical	Negative	25	2.2	484	$\pm$ 100
Copper Disc	Multi-Crystal	Vertical	Negative	50	2.2	484	$\pm$ 100
Paraboloid	Single-Crystal	Horizontal	Positive	25	1.8	324	$\pm$ 100
Paraboloid	Single-Crystal	Horizontal	Positive	50	1.8	324	$\pm$ 100
Paraboloid	Single-Crystal	Horizontal	Negative	25	1.8	324	$\pm$ 100
Paraboloid	Single-Crystal	Horizontal	Negative	50	1.8	324	$\pm$ 100

Note: Here the"Single-Crystal" superconductor type refers to the 31.5 mm diameter disc.

Table 3. Results summary of the impulses performed with the 1660 μF capacitor through the superconductors in liquid nitrogen. The acceleration standard deviation varies in the first decimal place, which is not shown.

Electrode Type	S/C Type	Orientation	Impulse Direction	Distance [cm]	Voltage [kV]	Discharge Energy [J]	Acceleration (3σ) [μg]
Copper Disc	Sintered	Horizontal	Positive	25	1.3	1402.7	± 48
Copper Disc	Sintered	Horizontal	Positive	50	1.3	1402.7	± 48
Copper Disc	Sintered	Horizontal	Negative	25	1.3	1402.7	± 48
Copper Disc	Sintered	Horizontal	Negative	50	1.3	1402.7	± 48
Copper Disc	Sintered	Vertical	Positive	25	1.3	1402.7	± 48
Copper Disc	Sintered	Vertical	Positive	50	1.3	1402.7	± 48
Copper Disc	Sintered	Vertical	Negative	25	1.3	1402.7	± 48
Copper Disc	Sintered	Vertical	Negative	50	1.3	1402.7	± 48
Paraboloid	Single-Crystal	Horizontal	Positive	25	1.1	1004.3	± 48
Paraboloid	Single-Crystal	Horizontal	Positive	50	1.1	1004.3	± 48
Paraboloid	Single-Crystal	Horizontal	Negative	25	1.1	1004.3	± 48
Paraboloid	Single-Crystal	Horizontal	Negative	50	1.1	1004.3	± 48

Note: Here the"Single-Crystal" superconductor type refers to the 45 mm diameter disc.

IV. Conclusions and Discussion

During the last two decades multiple groups have reported claims that superconductors could emit gravity-like beams when subjected to high intensity electrical current impulses. Our first set of trials gave only inconclusive results, which lead us to improve our experimental setup and our expertise. With our newly upgraded setup we achieved a more than satisfactory result that leads us to conclude the experiment series. We could draw the following conclusions:

2. The Claimed Gravity-Like Beam

In all our measurements we did not detect any change in acceleration during electric current impulses (of up to 6.5 kA) through various superconductor discs placed in liquid nitrogen within our measurement precision. The sensor used in all our measurements was a piezoelectric vibration sensor with a frequency range of 0-60 kHz. In all of the measurements reported by Poher and Schroeder the accelerometers had a significantly lower resonance frequency, which made the measurements inaccurate.

Our explanation for the cause of the signals previously reported by others is the influence of the emitted electromagnetic pulse on their sensors and data aquisition systems. We achieved a shielding of the EMP that allowed us to perform measurements without influencing our sensor. The new lower limit (3 σ) set for an acceleration change during the impulses as described in this paper is 100 μg for a peak current of 6.5 kA, a discharge voltage of 2.2 kV, a discharge energy of 484 J and an impulse duration of approx. 150 μs as well as 48 μg for a peak current of 4.3 kA, a discharge voltage of 1.3 kV, a discharge energy of 1402.7 J with an impulse duration of approx. 2 ms. We also performed measurements with a new type of electrode geometry that had a hollow parabolloid shape inside, resulting in a small (2 mm wide) contact circle at the edge of the supercondutor discs. We observed no difference in our results as compared to the measurements with the copper disc electrodes.

3. Recoil/Acousic Signal Analysis

We could observe that during the impulses through the superconductors spark erosion occurs within the contact region with the electrodes. This effect generates enough heat to vaporize the liquid nitrogen around the contact region. The quickly expanding nitrogen gas leads to a high machanical impulse that propagates through the support structure into the environment, which we measured as a high intensity acoustic signal with our accelerometers. Leading us to belive that the reported recoil effect is caused by the gas expansion originating from the contact region of the superconductor.

We have also determined that an impulse through an aluminium disc does not reproduce the same effects as an impulse through an YBCO superconductor since the spark erosion was absent. So the only way to perform an accurate control experiment is if the impulses are performed through the superconductor that is immersed in liquid nitrogen but its temperature is still well above its critical temperature (Tc). We performed numerous measurements under these conditions and concluded that the same acoustic signal is produced as compared to the case when the temperature fell below Tc.

V. Acknowledgment

We would like to thank Prof. Freudenberger / IFW Dresden for providing us with the capacitors and the high voltage charger. Further we would like to thank Dr. F. Werfel from the Adelwitz Technologiezentrum GmbH and G. Hathaway for providing us with the superconductor discs used during this experiment series.

References

[1] Podkletnov, E. and Modanese, G., "Investigation of High Voltage Discharges in Low Pressure Gases through Large Ceramic Superconducting Electrodes", Journal of Low Temperature Physics, 132(3/4) 2003, pp. 239-259

[2] Taylor, C.Y. and Modanese, G., "Evaluation of an impulse gravity generator based beamed propulsion concept", AIAA-2002-4095, 2002

[3] Poher, C., and Poher, D., Physical Phenomena Observed during Strong Electric Discharges into Layered Y123 Superconducting Devices at 77 K, APJ Vol3, Nr. 2, p51, November 2011, open access : http://dx.doi.org/10.5539/apr.v3n2p51

[4] Schroeder, D., http://starflight1.freeyellow.com/, 18th Decemer 2014

[5] Lőrincz, I., Tajmar, M., "Design and First Measurements of a Superconducting Gravity-Impulse-Generator", 51st AIAA/SAE/ASEE Joint Propulsion Conference, Volume: AIAA 2015-4080

[6] Podkletnov, E. and Nieminen, R., "A Possibility of Gravitational Force Shielding by Bulk $YBa_2Cu_3O_7$ Superconductor", Physica C, Vol. 203, pp. 441, 1992

[7] Poher, C., Poher, D., Marquet, P., "Propelling phenomenon revealed by electric discharges into layered Y123 superconducting ceramics", Eur. Phys. J. Appl. Phys. 50, 2010, pp. 30803

[8] Modanese, G., "A Comparison Between the YBCO Discharge Experiments by E. Podkletnov and C. Poher, and Their Theoretical Interpretations", Applied Physics Research, Vol. 5, No. 6, 2013

[9] http://www.universons.org/ (last access 07.2015)

[10] Poher, C., "Propelling device by means of matter particles acceleration, and applications of this device", Pub. No.: US 2010/0251717 A1, Oct. 7, 2010